Recent Progress in NEO-2 — A Code for Neoclassical Transport Computations Based on Field Line Tracing

Winfried KERNBICHLER[1]), Sergei V. KASILOV[1,2)], Georg O. LEITOLD[1]),
Viktor V. NEMOV[1,2)] and Klaus ALLMAIER[1])

[1)]*Association EURATOM-ÖAW, Institut für Theoretische Physik - Computational Physics,*
TU Graz, Petersgasse 16, A–8010 Graz, Austria
[2)]*Institute of Plasma Physics, National Science Center "Kharkov Institute of Physics and Technology",*
Akademicheskaya Str. 1, 61108 Kharkov, Ukraine

NEO-2 is a code for the computation of neoclassical transport coefficients and current drive efficiency in toroidal devices which is based on the field line integration technique. The possibility to use the complete linearized collision integral is realized in this code. In this report the results of comparison of the full matrix of transport coefficients in a tokamak with analytical models are presented. Effects of simplifications of the linearized collision model (e.g., reduction to a Lorentz model) are studied in order to provide a comparison with various momentum correction techniques used for the computation of transport coefficients in stellarators.

1. Introduction

Accurate computations of transport coefficients, bootstrap current and the generalized Spitzer function in tokamaks and stellarators is an important problem for stellarator optimization, generation of neoclassical data bases, and modeling of current drive. Based on the field line integration technique [1], the code NEO-2 has been developed for this purpose [2, 3]. This code solves the linearized drift kinetic equation in regimes where the effect of electric field on transport and bootstrap coefficients is negligible. Recently this code has been upgraded for computations of the full transport matrix and the possibility of treatment of magnetic fields in Boozer coordinates has been realized in addition to magnetic fields in real space coordinates. In the following, a comparison of NEO-2 results with results of analytical theory for tokamak are presented. Transport coefficients are computed here only for the electron component assuming the ions to be immobile.

2. Basic Equations

Approximating the energy dependence of the perturbation of the distribution function by the expansion over a finite number of test functions,

$$\delta f(\psi, s, v, \lambda) \approx f_0(\psi, v) \sum_{m=0}^{M} f_m(\psi, s, \lambda) \varphi_m(v/v_T) ,$$

$$\varphi_m(x) = \pi^{3/4} \sqrt{\frac{2\Gamma(m+1)}{\Gamma(m+5/2)}} L_m^{(3/2)}(x^2) , \qquad (1)$$

author's e-mail: winfried.kernbichler@TUGraz.at

where $f_0(\psi, v)$ is the Maxwellian and $L_m^{(3/2)}$ are associated Laguerre polynomials (Sonine polynomials) of the order $3/2$, the linearized drift kinetic equation (DKE) is transformed to a set of coupled two dimensional differential equations,

$$\sigma \frac{\partial f_m^\sigma}{\partial s} - \kappa \sum_{m'=0}^{M} \left\{ \nu_{mm'} \mathcal{L} f_{m'}^\sigma + \mathcal{K}_{mm'} f_{m'}^\sigma + \frac{1}{|\lambda|} D_{mm'} f_{m'}^\sigma \right\}$$
$$= \frac{\rho}{\langle |\nabla \psi| \rangle} \left(A_1 a_m^{(1)} + A_2 a_m^{(2)} \right) q_G^\sigma + A_3 a_m^{(3)} q_E^\sigma \qquad (2)$$

with the pitch-angle scattering operator

$$\mathcal{L} f_{m'}^\sigma = \frac{1}{2|\lambda|} \frac{\partial}{\partial \lambda} (1 - \lambda^2) \frac{\partial}{\partial \lambda} f_{m'}^\sigma(\psi, s, \lambda)$$
$$= 2 \frac{\partial}{\partial \eta} \left(\frac{\eta |\lambda|}{\hat{B}} \right) \frac{\partial}{\partial \eta} f_{m'}^\sigma(\psi, s, \eta) , \qquad (3)$$

and the integral part of the linearized collision operator

$$\mathcal{K}_{mm'} f_{m'}^\sigma = \frac{1}{|\lambda|} \sum_{\ell=0}^{L} I_{mm'}^\ell P_\ell(\lambda) \int_{-1}^{1} d\lambda' P_\ell(\lambda') f_{m'}^{\sigma'}(\psi, s, \lambda') , \qquad (4)$$

where P_ℓ are Legendre polynomials. Here, ψ is a flux surface label, s is the distance counted along the magnetic field line, $\lambda = v_\parallel / v$ is pitch, σ is the sign of $v_\parallel$, $\eta = (1 - \lambda^2) / \hat{B}$ is the normalized perpendicular invariant (magnetic moment), $\hat{B} = B / B_0$ is the magnetic field module normalized to a reference magnetic field B_0 which is equal to $(0, 0)$ harmonic of magnetic field expansion in Boozer coordinates, $B_0 = \langle B^3 \rangle / \langle B^2 \rangle$, $\kappa = 2 / l_c$ with $l_c = v_T \tau_{ee}$ being the mean free path, $\rho = v_T / \omega_c$, $v_T = (2T_e / m_e)^{1/2}$,

$\omega_c = eB_0 / m_e c$ and $\tau_{ee} = 3m_e^2 v_T^3 / \left(16\sqrt{\pi} n_e e^4 \Lambda\right)$ are electron Larmor radius, thermal velocity, cyclotron frequency and collision time, respectively, and $\langle \dots \rangle$ means the average over the volume between two neighboring magnetic surfaces (flux surface average). The quantities $\nu_{mm'}$, $I_{mm'}$, $D_{mm'}$ and $a_m^{(i)}$ are matrix elements independent of plasma parameters, whereas the quantities A_i are the thermodynamic forces defined as,

$$A_1 = \left(\frac{1}{n}\frac{\partial n}{\partial \psi} - \frac{3}{2T}\frac{\partial T}{\partial \psi} + \frac{e}{T}\frac{\partial \Phi}{\partial \psi}\right)\langle |\nabla \psi|\rangle,$$

$$A_2 = \frac{1}{T}\frac{\partial T}{\partial \psi}\langle |\nabla \psi|\rangle, \qquad A_3 = \frac{e}{T}\frac{\langle E_\parallel \hat{B}\rangle}{\langle \hat{B}^2\rangle}. \qquad (5)$$

The source terms q_G^σ and q_E^σ with drives by gradients and by parallel electric field, respectively, are defined as follows,

$$q_G^\sigma = \frac{\partial}{\partial \eta}\left(\frac{|\lambda|}{\hat{B}}\hat{V}_G\right), \qquad q_E^\sigma = \sigma \hat{B},$$

$$\hat{V}_G = \frac{1}{3}\left(\frac{4}{\hat{B}} - \eta\right)|\nabla \psi| k_G, \qquad (6)$$

where k_G is the geodesic curvature.

Equations (2) are discretized over the η variable on an adaptive non-equidistant grid and the resulting set of coupled ordinary differential equations is solved with help of integration along the field lines. In particular, all necessary flux surface averages are computed during this integration as follows,

$$\frac{\langle \alpha \rangle}{\langle \beta \rangle} = \lim_{L\to\infty}\int_0^L \frac{ds}{B}\alpha \ \Big/ \int_0^L \frac{ds}{B}\beta. \qquad (7)$$

As a result of computation, one obtains the matrix of transport coefficients L_{ij}^e defined through the thermodynamic forces A_j and thermodynamic fluxes I_i via

$$I_i = -\sum_{j=1}^{3} L_{ij}^e A_j, \qquad (8)$$

where $I_1 = \Gamma_e$, $I_2 = Q_e / T_e$ and $I_3 = \langle j_\parallel \hat{B}\rangle / e$. Here Γ_e and Q_e are average particle and heat flux densities defined as total particle and heat fluxes divided by the flux surface area and $j_\parallel$ is parallel electron current density.

Symmetric matrix L_{ij}^e is conveniently expressed through dimensionless coefficients γ_{ij} which depend only on the device geometry, the mean free path l_c and effective charge number Z as follows, $L_{ij} = n_e \gamma_{ij}\beta_i\beta_j / \tau_{ee}$, where $\beta_1 = \beta_2 = \rho$ and $\beta_3 = l_c$. For this purpose solution to (2) is formally presented as a superposition of thermodynamic forces,

$$f_m^\sigma = \frac{\rho}{\langle |\nabla \psi|\rangle}\left(A_1 \hat{f}_m^{\sigma,(1)} + A_2 \hat{f}_m^{\sigma,(2)}\right) + A_3 \hat{f}_m^{\sigma,(3)}. \qquad (9)$$

Then γ_{ij} are determined by normalized solutions for single drive problems, $\hat{f}_m^{\sigma,(i)}$, as follows

$$\gamma_{ij} = \frac{\alpha_i \alpha_j}{l_c}\sum_m \sum_{\sigma=\pm 1} b_m^{(i)}\left\langle \hat{B}\int_0^{1/\hat{B}} d\eta\, \hat{f}_m^{\sigma,(j)} q_i^{-\sigma}\right\rangle, \qquad (10)$$

where $q_1^\sigma = q_2^\sigma = q_G^\sigma$, $q_3^\sigma = q_E^\sigma$, $\alpha_1 = \alpha_2 = l_c\langle|\nabla\psi|\rangle^{-1}$, $\alpha_3 = 1$ and numerical coefficients $b_m^{(i)}$ are, again, independent of problem parameters. With help of these coefficients the quantity λ_{bb} [3] is expressed as $\lambda_{bb} = 2\gamma_{31}$.

It should be noted that matrices L_{ij}^e and γ_{ij} correspond to the effective radius r_{eff} used as a radial variable where $dr_{eff} = dV / S$, V is a volume limited by a flux surface and S is a flux surface area. In order to obtain these matrices for different definitions of plasma radius, e.g. for the radius defined via the toroidal flux, $r_\psi = (2\psi / B_{00})^{1/2}$, coefficients α_1 and α_2 should be multiplied with dr_ψ / dr_{eff}.

3. Computational Results

For the large aspect ratio tokamak with circular flux surfaces coefficients γ_{ij} computed by NEO-2 are compared to the analytical results of Refs. [4–6]. In particular, dimensionless transport coefficients for the Hinton and Hazeltine model [4], γ_{ij}^{HH}, are given by $\gamma_{ij}^{HH} = K_{ij}q^2\epsilon_t^{-3/2}Z_{eff}$ for $i, j = 1, 2$, $\gamma_{ij}^{HH} = K_{ij}q\epsilon_t^{-1/2} / 2$ for $i = 1, 2$ and $j = 3$ or $i = 3$ and $j = 1, 2$,

$$\gamma_{33}^{HH} = \frac{K_{33}\epsilon_t^{1/2} - 1}{2Z_{eff}\left(0.29 + 0.46\left(1.08 + Z_{eff}\right)^{-1}\right)}, \qquad (11)$$

and matrix K_{ij} is defined by Eqs. (6.125) and (6.126) of Ref. [4]. Here q is safety factor and $\epsilon_t = r/R$ is the inverse aspect ratio. The results of the comparison are presented in Figs. 1 and 2 for $t = 1/q = 0.362$ and $\epsilon_t = 0.075$. The results of NEO-2 are computed with associated Laguerre polynomials up to fourth order and Legendre polynomials up to third order. For all coefficients the dependence on collisionality as well as Z_{eff} is well reproduced. The main differences come from the finite toroidicity. Whereas NEO-2 does not assume smallness of the magnetic field modulation, theoretical approximations are based on the expansion over ϵ_t. It should be noted that in NEO-2 all nine transport coefficients are computed independently and Onsager symmetry of these coefficients is used for the control of the computation accuracy which improves with both, grid resolution and (mainly) number of Laguerre polynomials in modeling energy dependence. For the present computation violation of symmetries $\gamma_{13} = \gamma_{31}$ and $\gamma_{23} = \gamma_{32}$ is around 1 % and violation of symmetry $\gamma_{12} = \gamma_{21}$ is around 10 %.
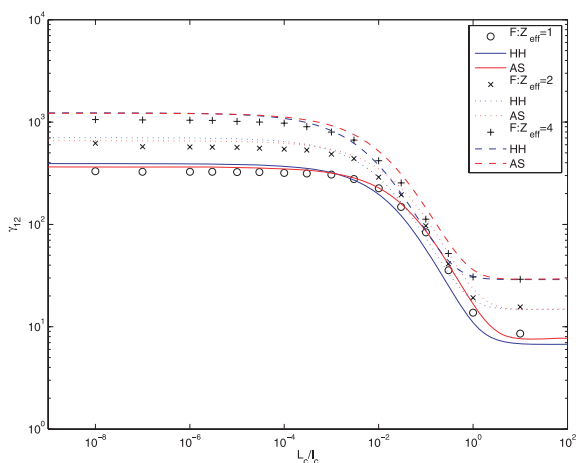
Beside the full linearized collision operator, two different model operators are used in Fig. 3, namely, the mono-energetic collision model and mono-energetic collision model with momentum recovery. Last two models are obtained by putting in (2) $D_{mm'} = I_{mm'}^\ell = 0$ or only $D_{mm'} = 0$, respectively. In particular, the mono-energetic model here corresponds to the most common mono-energetic approach where transport coefficients are given by the convolution over energy of the results for the Lorentz model. It can be seen that mono-energetic model overestimates particle diffusion coefficient γ_{11} while mono-energetic model with momentum recovery underes-
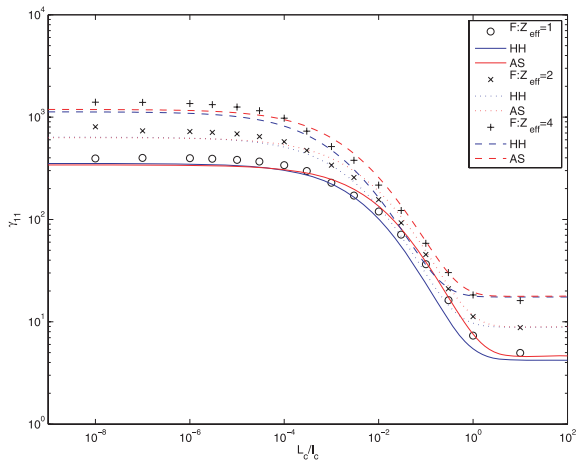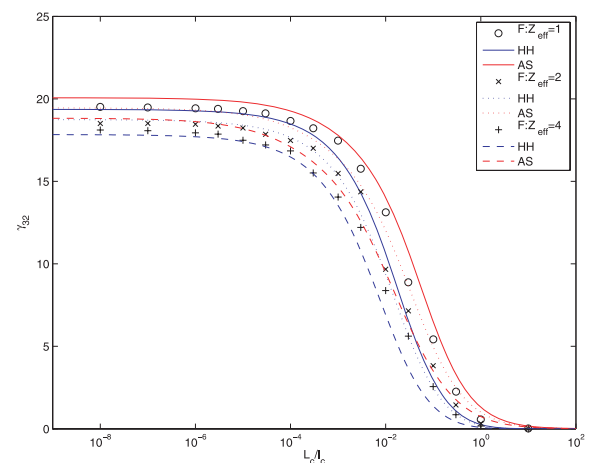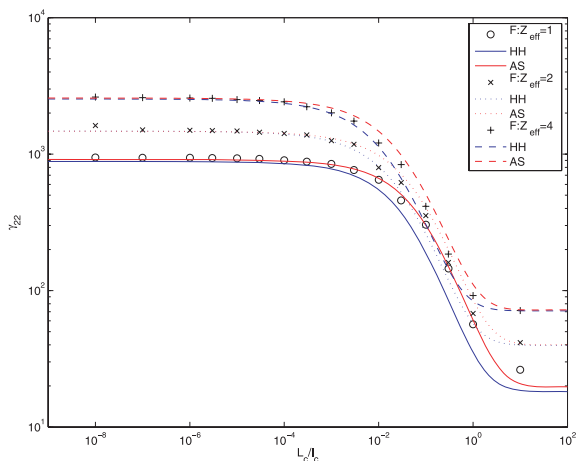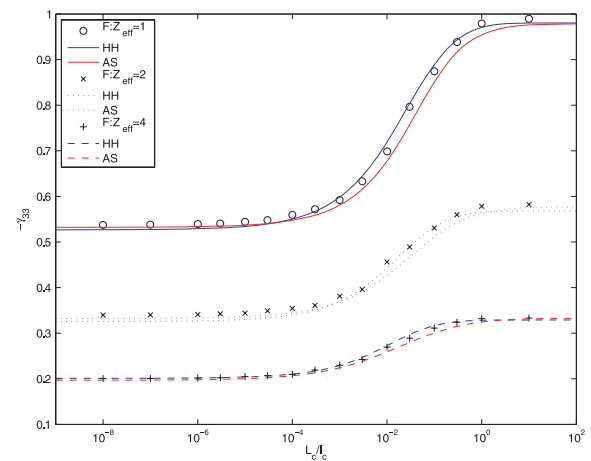
(a)
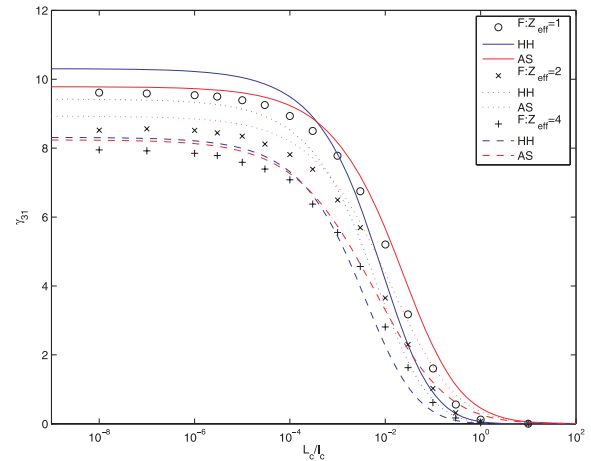
(a)

(b)

(b)

(c)

(c)

Fig. 1   Results of NEO-2 with full linearized collision operator (F) and analytical models of Ref. [4] (HH) and Refs. [5,6] (AS) for the dimensionless transport coefficients γ_{11} (a), γ_{12} (b) and γ_{22} (c), respectively, at three values of the effective charge Z_{eff}.

Fig. 2   The same as in Fig. 1 for the transport coefficients γ_{31} (a), γ_{32} (b) and $-\gamma_{33}$ (c), respectively.
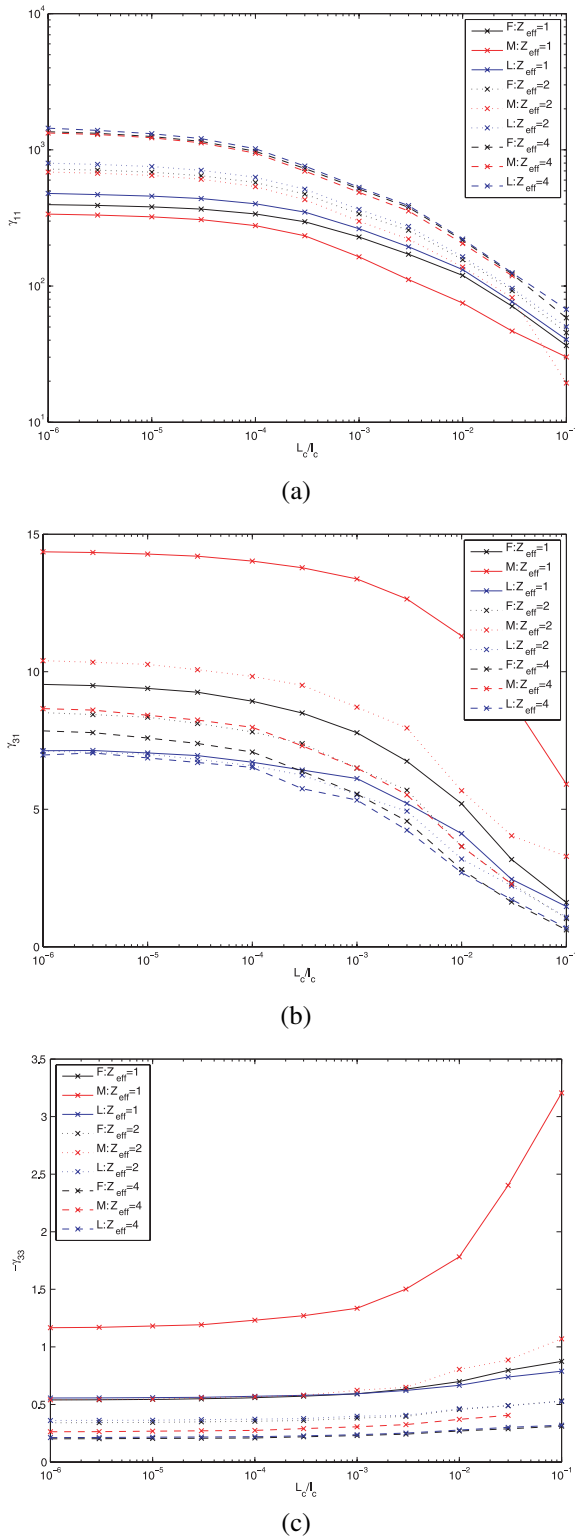
(a)

(b)

(c)

Fig. 3 Dimensionless particle diffusion coefficient γ_{11} (a), the bootstrap coefficient γ_{31} (b) and the conductivity coefficient $-\gamma_{33}$ (c), respectively, for the full linearized collision operator (F), mono-energetic approach (L) and mono-energetic approach with momentum recovery (M).

timates this coefficient as compared to the full linearized collision model. The bootstrap coefficient γ_{31}, in turn, is underestimated by the mono-energetic model while the mono-energetic model with momentum recovery overestimates it. Finally, conductivity coefficient is well reproduced by the mono-energetic model while the mono-energetic model with momentum recovery significantly overestimates it. Differences between all three models are naturally reduced with higher Z_{eff}. Currently NEO-2 has been and is being used for the benchmarking of various methods for the computation of mono-energetic transport coefficients and bootstrap coefficient [7, 8] as well as momentum correction techniques [9].

Acknowledgments

[1] V.V. Nemov, S.V. Kasilov, W. Kernbichler and M.F. Heyn, Phys. Plasmas **6**, 4622 (1999).

[2] W. Kernbichler, S.V. Kasilov, G.O. Leitold, V.V. Nemov and K. Allmaier, *Proc. of the 15th Int. Stellarator Workshop*, Madrid, 3-7 October 2005, P2-15 (2005).

[3] W. Kernbichler, S.V. Kasilov, G.O. Leitold, V.V. Nemov and K. Allmaier, *33rd EPS Conference on Plasma Physics, Rome*, 19-23 June 2006, ECA Vol. **30I** P-2.189 (2006).

[4] F.L. Hinton and R.D. Hazeltine, Rev. Mod. Phys **48**, 239 (1976).

[5] O. Sauter, C. Angioni and Y.R. Lin-Liu, Phys. Plasmas **6**, 2834 (1999).

[6] C. Angioni and O. Sauter, Phys. Plasmas **7**, 1224 (2000).

[7] K. Allmaier *et al.*, *Proc. of the 16th International Stellarator/Heliotron Workshop*, Ceratopia Toki, Gifu, Japan, 15-19 October 2007, P2-029 (2007).

[8] K. Allmaier *et al.*, *Proc. of the 16th International Stellarator/Heliotron Workshop*, Ceratopia Toki, Gifu, Japan, 15-19 October 2007, P2-021 (2007).

[9] C.D. Beidler *et al.*, *Proc. of the 16th International Stellarator/Heliotron Workshop*, Ceratopia Toki, Gifu, Japan, 15-19 October 2007, P2-030 (2007).